

NOON states from cavity-enhanced down-conversion: High quality and super-resolution

Florian Wolgramm, Alessandro Cerè, and Morgan W. Mitchell

ICFO - Institut de Ciències Fotoniques, Mediterranean Technology Park, 08860 Castelldefels (Barcelona), Spain

(Dated: 27 November 2009)

Indistinguishable photons play a key role in quantum optical information technologies. We characterize the output of an ultra-bright photon-pair source using multi-particle tomography [R. B. A. Adamson et al., Phys. Rev. Lett. **98**, 043601 (2007)] and separately identify coherent errors, decoherence, and distinguishability. We demonstrate generation of high-quality indistinguishable pairs and polarization NOON states with 99% fidelity to an ideal NOON state. Using a NOON state we perform a super-resolving angular measurement with 90% visibility.

PACS numbers: 42.50.Dv, 03.65.Ud, 42.65.Yj, 42.25.Hz

Many applications in quantum information, quantum imaging and quantum metrology rely on the availability of high-quality single photons or entangled photon pairs. Depending on the kind of application, the requirements on a source of photonic quantum states include brightness and efficiency as well as the degree of indistinguishability, purity and entanglement of the output state. Recently there has been increasing interest in the generation of cavity-enhanced paired photons [1, 2, 3, 4, 5, 6, 7, 8], because the cavity geometry enhances the photon generation into the spatial and spectral resonator modes increasing at the same time brightness, collection efficiency and indistinguishability. The enhancement of the brightness is of the order of the cavity finesse [4]. When the nonlinear crystal is type-II phase-matched, it is possible to achieve polarization entanglement and create NOON states that can be applied to achieve phase super-resolution. Due to multiple passage through the crystal, such cavity schemes are more sensitive to imperfections in materials and alignment. Another challenge is double resonance that is not automatically achieved since in a type-II process the two generated photons have orthogonal polarization and see different refractive indices in the birefringent nonlinear crystal. Due to these cavity effects type-II schemes can suffer from a low Hong-Ou-Mandel (HOM) dip visibility [9], e.g. in [4], where the reported visibility was 76.8% and not all reasons for the low visibility could be identified. A limited visibility can be caused by distinguishing timing information, coherent state-preparation errors, and decoherence. These three possibilities cannot be differentiated by a HOM measurement. Nevertheless, multi-particle states can be fully characterized, including decoherence and distinguishability of particles by tomographic techniques [10]. We apply these techniques to the output pairs from a cavity-enhanced down-conversion source, and show that cavity-enhanced down-conversion not only provides a large photon flux, but is also capable of producing highly indistinguishable photons that can be used to create interesting and useful quantum states such as a high-fidelity NOON state.

The experimental setup consists of two parts, one for the preparation of the state and the other for its analysis. The state preparation part is based on the high-brightness cavity-enhanced down-conversion source described in detail in a previous publication [7]. As principal light source we use a single-frequency diode laser locked to the D_1 transition of atomic rubidium at 795 nm (Figure 1). The frequency doubled part of the laser pumps a type-II phase-matched PPKTP crystal inside an optical cavity. After the photons leave the cavity, a variable retarder consisting of a polarizing beam splitter, two quarter wave plates and two mirrors in a Michelson geometry produces a relative delay between the H - and V -polarized photons.

A general polarization analyzer, consisting of a quarter wave plate (QWP1) followed by a half wave plate (HWP) and a polarizing beam splitter (PBS2) is used to determine the measurement basis as shown in Figure 1. To generate a NOON state in the H/V basis another quarter wave plate (QWP2) can be added. The two output ports of PBS2 are coupled to single-mode fibers and split with 50:50 fiber beam splitters. The four outputs are connected to a set of single photon counting modules (Perkin Elmer SPCM-AQ4C). Time-stamping was performed by coincidence electronics with a resolution of 2 ns. By considering a time window of 150 ns, that is longer than the coherence time of each individual photon, we can evaluate the coincidences between any two of the four channels.

To observe a classic “HOM dip”, we set the analyzer for ± 45 degree with QWP1 and QWP2 removed and scan the relative delay. The resulting curve is shown in Figure 2. Accidental counts due to probabilistic photon arrival times that account for approximately 10% of the coincidence counts out of the dip have been subtracted. For zero delay the photons are highly indistinguishable indicated by a visibility of the graph of 96%. With reduced pump power, similar visibilities were seen without need for accidentals subtraction.

We use the multi-particle state tomography of reference [10]. As in tomographic characterization of qubits [11],

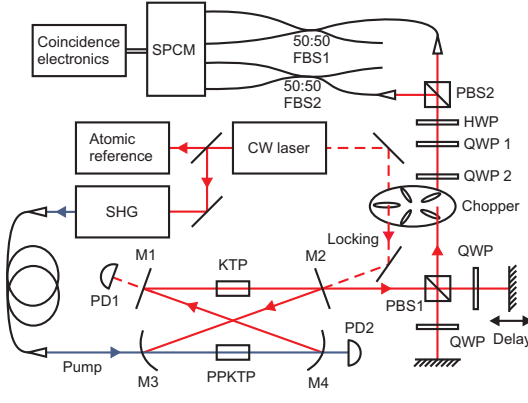


FIG. 1: Experimental Setup. SHG, second harmonic generation cavity; PPKTP, phase-matched nonlinear crystal; KTP, compensating crystal; M1-4, cavity mirrors; PBS, polarizing beam splitter; HWP, half wave plate; QWP, quarter wave plate; SMF, single-mode fiber; PD, photodiode; FBS, fiber beam splitter; SPCM, single photon counting module.

this method gives a complete description of the polarization of the photons, including partial coherence. Moreover, it quantifies the operational distinguishability of the photons, i.e., information in unobserved degrees of freedom that could in principle be used to identify the photons, and which destroys non-classical interference. For example, photons which differ in arrival time, frequency, or spatial mode are operationally distinguishable and do not show non-classical interference. The presence of these other degrees of freedom allows the photons to have any symmetry of their polarization wave-function while remaining globally symmetric. Using the symmetry-ordered basis $\{|H_1 H_2\rangle, |\psi^+\rangle, |V_1 V_2\rangle, |\psi^-\rangle\}$, with $|\psi^\pm\rangle \equiv (|H_1 V_2\rangle \pm |V_1 H_2\rangle)/\sqrt{2}$, a general polarization state is described by a density matrix of the form

$$\rho = \begin{pmatrix} \begin{pmatrix} \rho_S \end{pmatrix} & \begin{pmatrix} \cdot \\ \cdot \\ \cdot \end{pmatrix} \\ \begin{pmatrix} \cdot \\ \cdot \\ \cdot \end{pmatrix} & \begin{pmatrix} \rho_A \end{pmatrix} \end{pmatrix}, \quad (1)$$

where ρ_S is a 3×3 matrix describing the symmetric portion of the polarization state and ρ_A is a 1×1 matrix describing the anti-symmetric portion. Coherences (\cdot), between these parts are, by assumption, unobservable and do not contribute to any measurable outcome. We now calculate the coincidence probability for an arbitrary state ρ , and also for the same state with the photons made distinguishable. Applied to the state at the center of a HOM dip, these give the HOM visibility. We assume that the analyzer is set to discriminate in the basis $|\alpha\rangle, |\beta\rangle \equiv (|H\rangle \pm \exp[i\phi]|V\rangle)/\sqrt{2}$, so that a coincidence indicates a state with one α and one β photon. Within the symmetric(anti-symmetric) subspace, the coincidence detection is then a projection onto $(|\alpha_1 \beta_2\rangle \pm |\beta_1 \alpha_2\rangle)/\sqrt{2}$. For the symmetric subspace this

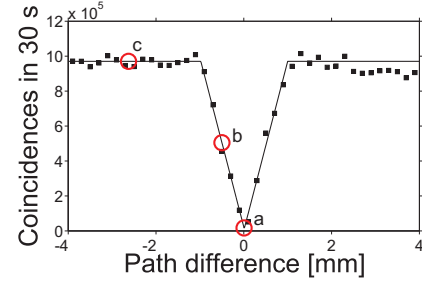


FIG. 2: Hong-Ou-Mandel effect. Experimental data and triangular fit function. Labelled points indicate locations of tomographic reconstructions in Figure 3.

state is $(|H_1, H_2\rangle - \exp[2i\phi]|V_1, V_2\rangle)/\sqrt{2}$, for the anti-symmetric subspace, it is $|\psi^-\rangle$ itself. In terms of the density matrix ρ , the coincidence probability is then

$$C = \rho_{44} + \frac{1}{2}(\rho_{11} + \rho_{33}) - \text{Re}[e^{2i\phi}\rho_{13}]. \quad (2)$$

We can also transform this state into one with complete in-principle distinguishability, by setting $\rho_{44} = \rho_{22} = (\rho_{22} + \rho_{44})/2$. Physically, this transformation can be accomplished by introducing a large delay between the photons. Using $\text{Tr}[\rho] = 1$ we find

$$C_{\text{dist}} = \frac{1}{2} - \text{Re}[e^{2i\phi}\rho_{13}]. \quad (3)$$

If C is the probability at the center of the HOM dip, i.e., for the state with maximal indistinguishability, then the visibility of the HOM dip is

$$V_{\text{HOM}} \equiv \frac{C_{\text{dist}} - C}{C_{\text{dist}} + C} = \frac{\rho_{22} - \rho_{44}}{2 - (\rho_{22} - \rho_{44}) - 4\text{Re}[e^{2i\phi}\rho_{13}]}. \quad (4)$$

We note that this depends on few of the density matrix elements, and thus a variety of different states could have the same HOM dip visibility.

We can also calculate the visibility in an interferometric measurement based on polarization rotations, such as those which give super-resolution. We assume a wave plate or other optical device applies a unitary rotation to both photons of the state, and they are detected in the α, β state as above. The ψ^- component is invariant under any unitary transformation affecting both photons, and thus contributes a constant ρ_{44} to the coincidence probability. In contrast, the contribution of the triplet component may oscillate between zero and $\rho_{11} + \rho_{22} + \rho_{33} = 1 - \rho_{44}$. A limit on interferometric visibility is thus

$$V_{\text{INT}} \leq \frac{1 - \rho_{44}}{1 + \rho_{44}}. \quad (5)$$

We follow the tomography method developed in [10, 12] in order to get a polarization characterization of the

output state. We evaluated the coincidence counts for the same 10 different wave plate settings of HWP and QWP1 as in [10]. The acquisition time for each wave plate setting was 60 seconds. Applying a maximum likelihood reconstruction we obtain the polarization density matrix. The single count rate corrected for accidentals during the measurements was typically 10 000 counts/s. We measured the density matrix for different delays between the photons corresponding to different positions in the HOM dip. We generated different states as follows: a) center of dip b) mid-point of dip c) outside of dip. In addition, we produced an unknown state d) by tuning the fundamental laser by about 3.1 GHz from the frequency used in a) – c). At this detuning we observe a reduced HOM visibility, for reasons that are not understood. Data for d) were taken at the center of the dip, i.e., with zero relative delay. For all these states we applied the same tomography procedure. Figure 3 shows the elements of the real parts of the density matrices. The imaginary parts are close to zero and are not shown.

We note that the populations in $|\psi^+\rangle$ and $|\psi^-\rangle$ change for different dip positions: a) 94% and 4%, b) 68% and 28%, c) 49% and 50%, d) 66% and 16%. We also note that while b) and d) have a similar amount of HOM dip visibility, their density matrices look very different. In b) only the ψ^+ and ψ^- populations are significant, while d) shows also VV population and coherence between ψ^+ and VV . Thus b) shows distinguishability while d) shows some distinguishability but also decoherence and coherent errors which cause non-zero off-diagonal elements to appear in the density matrix. This shows clearly that multi-particle tomography provides information not present in the HOM visibility, and can be

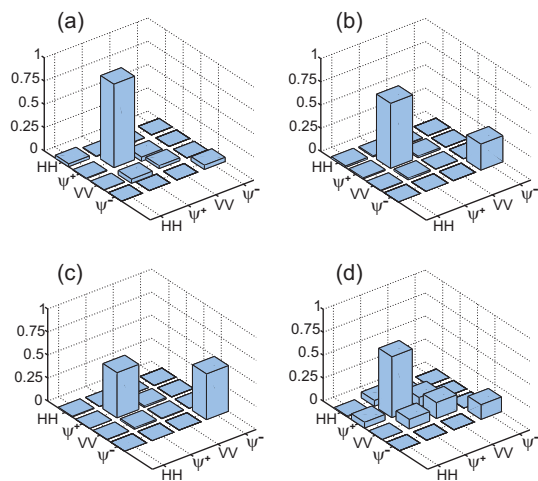


FIG. 3: Reconstructed polarization density matrices for (a) center of HOM dip, (b) edge of HOM dip, (c) outside of HOM dip (corresponding to points in Figure 2), (d) center of dip, but with system tuned to a different frequency.

useful for identifying imperfections in generated states. The achieved high visibility of the state is the requirement for a high-fidelity NOON state. We introduce another quarter wave plate (QWP2) before the analyzing part of the setup to create a two-photon NOON state in the H/V basis, which can be written $1/\sqrt{2}(|H_1, H_2\rangle + e^{i\phi}|V_1, V_2\rangle)$. Since the output state of the cavity $|HV\rangle$ is already a NOON state in the circular basis $|HV\rangle = i/\sqrt{2}(|L_1, L_2\rangle + |R_1, R_2\rangle)$, this state can be transferred into a NOON state in the H/V basis by sending it through an additional quarter wave plate at 45 degrees. In Figure 4 real and imaginary parts of the reconstructed density matrix of a NOON state are displayed. The coherence of the state is partly imaginary leading to a phase of $\phi = 0.20$ between HH and VV components (Figure 4(b)), which is however of no importance in the following. The fidelity of this state with the corresponding ideal two-photon NOON state $1/\sqrt{2}(|H_1, H_2\rangle + e^{i\phi}|V_1, V_2\rangle)$ is 99%, making the state suitable for applications such as phase-estimation [13]. To demonstrate this ability, we performed a super-resolving phase experiment. After passing the NOON state, for this experiment in the circular basis (without QWP1 and QWP2), through the HWP, the coincidence counts between the output ports of PBS2 for different HWP settings were recorded. In Figure 5 the interference fringes of the coincidences are displayed together with single counts from a measurement in which one polarization of the cavity output was blocked. The period of the coincidence counts oscillations is shorter by a factor of two compared to the singles, as expected for a two-photon NOON state. The sinusoidal fit function of the coincidences shows a high visibility of 90%.

We have used quantum state tomography to analyze the pair-photon state from a cavity-enhanced down-conversion source in order to optimize the indistinguishability of the photons. The highly indistinguishable photons have then been converted to a high-fidelity polarization NOON state in the H/V basis. Furthermore, a phase super-resolution measurement using NOON states has been demonstrated showing that these states are suitable for applications in quantum imaging and atomic

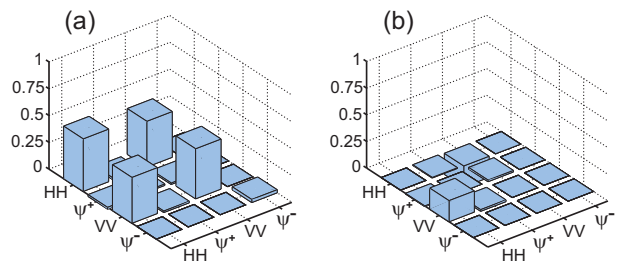


FIG. 4: (a) Real and (b) imaginary part of the polarization density matrix of the pair-photon state transformed to a two-photon NOON state.

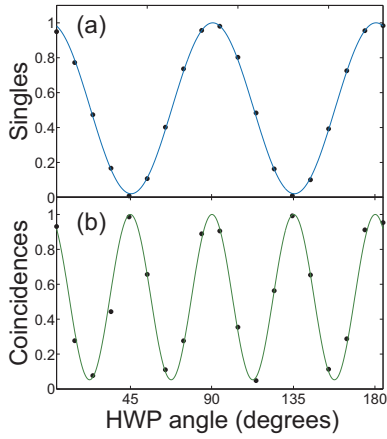


FIG. 5: (a) Standard phase measurement. Normalized singles detection at the transmitted port of PBS2. In this measurement only the H polarized part of the pair-photon state was sent to the analyzer. (b) Super-resolving phase measurement. Normalized coincidence detection between reflected and transmitted port of PBS2 for a NOON state input. The shorter period of the coincidence counts oscillations indicates super-resolution.

spectroscopy. For the cavity-enhanced down-conversion source used in this experiment, applications in atomic spectroscopy are especially promising since the photon wavelength is at a rubidium resonance. In addition, the photons are spectrally tailored, such that even after filtering them to a bandwidth of a few MHz, which is comparable to the natural linewidth of atomic rubidium, a high count rate of 70 pairs/(s mW MHz) is expected [7, 14].

We thank R. B. A. Adamson and R. L. Kosut for help on the reconstruction code as well as X. Xing, A. M. Steinberg and A. Predojević, who participated in early work for this experiment. In addition we want to thank Y. de Icaza Astiz for useful discussions. This work was supported by the Spanish Ministry of Science and Innovation under the Consolider-Ingenio 2010 Project “Quantum Optical Information Technologies” and the ILUMA project (Ref. FIS2008-01051) and by an ICFO-OCE collaborative research program. F. W. is supported by the Commission for Universities and Research of the Department of Innovation, Universities and Enterprises of the Catalan Government and the Euro-

pean Social Fund.

-
- [1] Z. Y. Ou and Y. J. Lu, “Optical parametric oscillator far below threshold: Experiment versus theory,” *Phys. Rev. Lett.* **83**, 2556–2559 (2000).
 - [2] Y. J. Lu, R. L. Campbell, and Z. Y. Ou, “Mode-locked two-photon states,” *Phys. Rev. Lett.* **91**, 163602 (2003).
 - [3] H. Wang, T. Horikiri, and T. Kobayashi, “Polarization-entangled mode-locked photons from cavity-enhanced spontaneous parametric down-conversion,” *Phys. Rev. A* **70**, 043804 (2004).
 - [4] C. E. Kuklewicz, Ph.D. thesis, Massachusetts Institute of Technology, 2005.
 - [5] C. E. Kuklewicz, F. N. C. Wong, and J. H. Shapiro, “Time-bin-modulated biphotons from cavity-enhanced down-conversion,” *Phys. Rev. Lett.* **97**, 223601 (2006).
 - [6] M. Scholz, F. Wolfgramm, U. Herzog, and O. Benson, “Narrow-band single photons from a single-resonant optical parametric oscillator far below threshold,” *Appl. Phys. Lett.* **91**, 191104 (2007).
 - [7] F. Wolfgramm, X. Xing, A. Cerè, A. Predojević, A. M. Steinberg, and M. W. Mitchell, “Bright filter-free source of indistinguishable photon pairs,” *Opt. Express* **16**, 18145–18151 (2008).
 - [8] X.-H. Bao, Y. Qian, J. Yang, H. Zhang, Z.-B. Chen, T. Yang, and J.-W. Pan, “Generation of Narrow-Band Polarization-Entangled Photon Pairs for Atomic Quantum Memories,” *Phys. Rev. Lett.* **101**, 190501 (2008).
 - [9] C. K. Hong, Z. Y. Ou, and L. Mandel, “Measurement of subpicosecond time intervals between two photons by interference,” *Phys. Rev. Lett.* **59**, 2044–2046 (1987).
 - [10] R. B. A. Adamson, L. K. Shalm, M. W. Mitchell, and A. M. Steinberg, “Multiparticle state tomography: Hidden differences,” *Phys. Rev. Lett.* **98**, 043601 (2007).
 - [11] D. F. V. James, P. G. Kwiat, W. J. Munro, and A. G. White, “Measurement of qubits,” *Phys. Rev. A* **64**, 052312 (2001).
 - [12] R. B. A. Adamson, P. S. Turner, M. W. Mitchell, and A. M. Steinberg, “Detecting hidden differences via permutation symmetries,” *Phys. Rev. A* **78**, 033832 (2008).
 - [13] M. W. Mitchell, J. S. Lundeen, and A. M. Steinberg, “Super-resolving phase measurements with a multiphoton entangled state,” *Nature (London)* **429**, 161–164 (2004).
 - [14] A. Cerè, V. Parigi, M. Abad, F. Wolfgramm, A. Predojević, and M. W. Mitchell, “Narrowband tunable filter based on velocity-selective optical pumping in an atomic vapor,” *Opt. Lett.* **34**, 1012–1014 (2009).